The 5th IEEE International Conference on E-Health and Bioengineering - EHB 2015
Grigore T. Popa University of Medicine and Pharmacy, Iaşi, Romania, November 19-21, 2015

Feature Ensemble for Quantitative Analysis of Emphysema in CT imaging

Rodrigo Nava*, Jimena Olveres†, Jan Kybic*, Boris Escalante†, and Gabriel Cristóbal‡
*Faculty of Electrical Engineering, Czech Technical University in Prague
Czech Republic
Email: uriel.nava@gmail.com
†Facultad de Ingeniería, Universidad Nacional Autónoma de México (UNAM)
Mexico City, Mexico
‡Instituto de Óptica, Spanish National Research Council (CSIC)
Madrid, Spain

***Abstract*—Chronic obstructive pulmonary disease is a non-reversible disorder characterized primarily by a dominant emphysema or bronchitis. Since early treatments can help to control the symptoms, the quantification of emphysema has become an important topic. Here, we introduce a novel procedure to quantify emphysematous lesions using an ensemble of features based on log-Gabor filters, mean difference technique, and intensity values. This set captures both spatial and frequency variations and provides a suitable description of lung tissue. Leave-patient-out cross-validation was employed on the computed tomography emphysema database to validate our proposal. The sensitivity and specificity achieved were 91.22% and 95.48%, respectively. Such results have demonstrated that the proposed methodology could assist in quantification of emphysema.**

***Keywords*—Emphysema, feature ensemble, log-Gabor filters, mean difference technique, quantitative CT.**

I. Introduction

According to the Global Initiative for Chronic Obstructive Lung Disease, chronic obstructive pulmonary disease (COPD) is a common, preventable, and treatable disease. COPD is characterized by a persistent airflow limitation, which is caused by a mixture of diseases of small airways and parenchymal destruction. It is emerging as a worldwide health problem and is expected to be responsible of 10% of the World's mortality by 2030 [1].

Emphysema is the most common manifestation of COPD. The condition causes permanent abnormal enlargement of air spaces by dilatation of the alveoli and destruction of their walls [2]. Three subtypes of emphysema can be recognized: panlobular (PL) that appears predominantly at the lower half of the lungs; centrilobular (CL), which is the most common type of emphysema, it begins in the bronchioli and spreads peripherally; and paraseptal (PS) that is localized around the pleura.

Computed tomography (CT) imaging is an important aid in the accurate detection and diagnosis of emphysema because it offers high-contrast and high-resolution details of lungs and airways [3]. Detection of emphysema is performed by counting the number of voxels below a threshold. Typically, around -950 Hounsfield units [4]. However, this method fails to detect the pathology at an early stage and does not allow to discriminate pathological sub-phenotypes of emphysema [5]. Hence, a more powerful quantitative analysis of emphysematous tissue is a crucial key to determine the stage of COPD and enable individualized treatments.

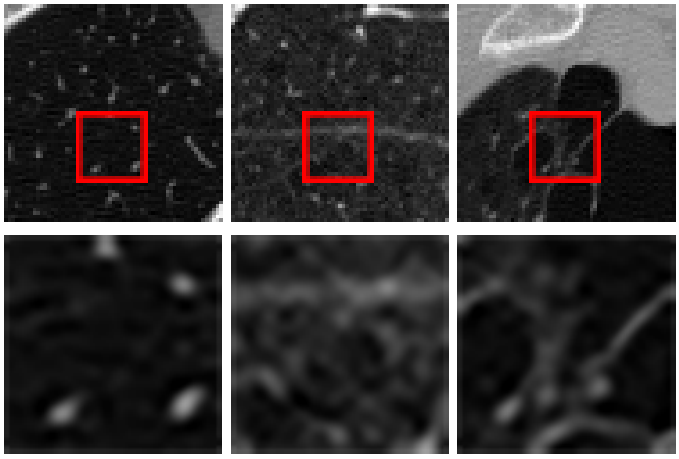

(a) (b) (c)

Figure 1. First row shows lung tissue ROIs from the computed tomography emphysema database [6]. Second row shows red squares drawn and magnified by a factor of 4. **(a)** NT; **(b)** CL; and **(c)** PS.

Several attempts to characterize emphysematous tissue have been made but still new techniques are constantly tested in order to improve results. In [6], Sørensen et al. described emphysema using a combined model based on local binary patterns (LBPs) [7] and intensity histograms on small patches. Nava et al. [5] introduced an extended model based on complex Gabor filters and LBPs. In [8], emphysema features were computed using Markov random fields, whereas Azim et al. [9] used a probabilistic model and the kernel Fisher method with relative success. All the aforesaid methods used the computed tomography emphysema database to validate their proposals.

978-1-4673-7545-0/15/$31.00

In addition to the abnormal low attenuation areas in lung parenchyma, it is necessary to consider textural appearance to refine the differential diagnosis. Emphysematous tissue contains more edges and homogeneous attenuation areas than normal tissue (NT) [6], CL produces small circular areas of lung destruction [10], and PS causes a relatively reduced attenuation at subpleural areas [11], (see Fig. 1).

The aim of this study is to propose a model that captures both textural variations and intensity information. Hence, an approach for emphysema characterization using log-Gabor filters (LGFs) [12], mean difference technique (MDY) [13], and intensity histograms is introduced.

Since micro structures may appear at different scales, it is necessary a multi-scale analysis. LGFs provide a description of spatial variations in specific orientations and frequency bands. Furthermore, they also possess a strong correlation with the human visual system that makes them suitable for detecting salient edges. On the other hand, MDY is a powerful tool used to describe the complexity of 1D signals and represents a general approach for texture analysis. Here, it is used as a measure of emphysema variations. Finally, the intensity information was included as a histogram.

This proposal combines the three descriptors into a feature ensemble and provides a robust description of emphysema by taking advantage of a time-frequency representation and spatial information.

II. Computed tomography emphysema database

In order to validate the proposal, we used the database provided in [6] that consists of 168 non-overlapping ROIs of size 61 $\times$ 61 pixels, annotated in 25 subjects manually and divided into three groups: healthy non-smokers, smokers without COPD, and smokers with moderate or severe COPD. These ROIs belong to three patterns: NT (59 ROIs from 8 subjects), PS (59 ROIs from 10 subjects), and CL (50 ROIs from 7 subjects). The NT ROIs were extracted from healthy non-smokers, whereas the CL and PS samples were extracted from both smokers with and without COPD. Note that the database excludes PL samples.

We followed recommendations in [6] and considered samples of size 31 $\times$ 31 by removing pixels on all sides, so that, the size fits the physical extent of emphysema within the secondary lobule.

III. Methodology

Feature extraction is performed through LGF, MDY, and intensity histograms. Then, principal component analysis (PCA) is applied to reduce dimensionality and remove redundant information. The proposal uses the most significant components. The parameters are optimized based on the classification accuracy. Finally, a random forest classifier is trained using leave-patient-out cross-validation.

A. Log-Gabor filters

LGFs [12] are an improved version of the classic Gabor filters. They are defined in the frequency domain as Gaussian functions that are shifted from the origin. The natural logarithm applied to the radial component minimizes the DC offset and distributes the frequency bands in a better way, namely, the overlapping between bands is minimized, (see Fig. 2).

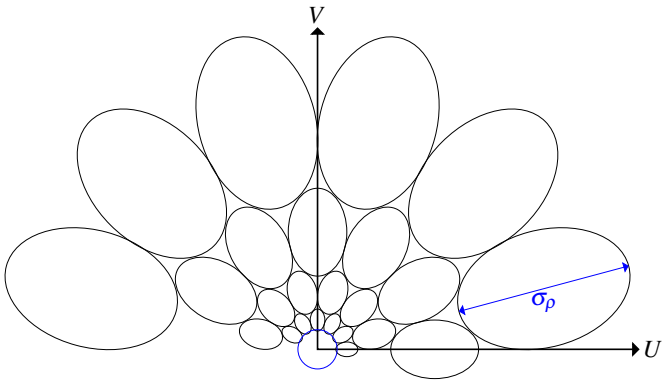

Figure 2. Log-Gabor filter bank. The contours are shown at full-width at half-amplitude. The scales σ_ρ are separated by one octave.

A 2D log-Gabor filter $G(\rho,\theta)$ in the frequency domain can be expressed as:

$$G_{u_0,\theta_0}(\rho,\theta) = e^{-\frac{1}{2}\left[\frac{\log\left(\frac{\rho}{u_0}\right)}{\log\left(\frac{\sigma_\rho}{u_0}\right)}\right]^2} e^{-\frac{1}{2}\left[\frac{(\theta-\theta_0)}{\sigma_\theta}\right]^2} \tag{1}$$

where $\rho = \sqrt{x^2+y^2}$ and $\theta = \tan^{-1}(y/x)$ represent the polar coordinates, u_0 is the central frequency, θ_0 is the orientation angle, and σ_ρ and σ_θ characterize the scale- and angular-bandwidth respectively.

According to [14], we build a filter bank composed of 24 filters distributed over four scales: $\{2^{i-0.5}\sqrt{(2)}|i=1,\ldots,4\}$ and six orientations: $\{\frac{k\pi}{6}|k=0,\ldots,5\}$. Even scales were rotated by a constant factor consisting of the half a distance between filter centers to better cover the Fourier plane, (see Fig. 2).

Given an emphysematous ROI, $r(x,y)$, its log-Gabor filtered response is:

$$J_{u_0,\theta_0}(x,y) = \mathscr{F}^{-1}\left\{\mathscr{F}\{r(x,y)\}\, G_{u_0,\theta_0}(\rho,\theta)\right\} \tag{2}$$

where $\mathscr{F}$ represents the Fourier transform.

To overcome the rotation variance drawback, for each scale, $i=1,\ldots,4$, we propose to keep the filtered response with the maximum energy as follows:

$$K_i(x,y) = MAX\left\{J_{i,\theta}(x,y), \forall\theta\right\} \tag{3}$$

The first four central moments: mean, μ, standard deviation, σ, skewness, γ, and contrast, $C = \sigma/\kappa^{0.25}$ where κ is kurtosis, are used to construct the log-Gabor feature vector, $\overline{LG}$.

$$\begin{aligned}\overline{LG} = &[\mu(K_1(x,y)), \sigma(K_1(x,y)), \gamma(K_1(x,y)), C(K_1(x,y)), \ldots,\\ &\mu(K_4(x,y)), \sigma(K_4(x,y)), \gamma(K_4(x,y)), C(K_4(x,y))]\end{aligned} \tag{4}$$

therefore, the $\overline{LG}$ vector is 16-dimensional.

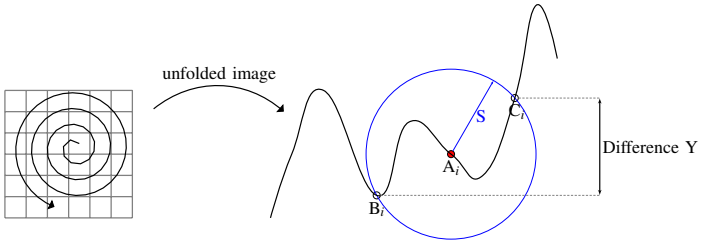

Figure 3. Schematic illustration of the Difference Y with respect to a single point A given a scale S. The difference is determined by the points B and C.

B. Mean difference technique

Originally proposed by Andrle [13] to describe the complexity of geomorphic lines; it has been further extended by Huang and Esbensen [15].

The algorithm unfolds the image into a one-dimensional signal. Since the simplest row-by-row unfolding does not allow to trace structures and keep spatial relations, we performed this operation using a spiral path. Such an unfolding method allows to analyze textures in a similar manner to LBPs. Then, N points are selected randomly along the unfolded image. Here, due to the size of the images, we set $N = 400$. For each point, circles of radius S are constructed and the intersections with the signal are computed, see Fig. 3.

The MDY is calculated by averaging all individual differences that belong to a single scale. By repeating this operation for all possible scales $S = 1,\ldots,M/2$ where M is the size of the image, it is possible to build a feature vector that characterizes the signal periodicity. The parameter S introduces the notion of scale in the domain of the signal. The firsts scales may concentrate noise information, whereas large scales may not contain neighboring information. Hence, we only used scales $S = \{3,\ldots,8\}$:

$$MDY(S) = \frac{1}{N}\sum_{i=1}^{N} |C_i - B_i|_S \tag{5}$$

where C and B are corresponding intersections with the signal. The final vector is 6-dimensional.

Another complementary measure that can be extracted with this technique is the mean angle although it was not used in the present study.

C. Intensity histogram

According to [5], [6], [16], it is necessary to incorporate intensity information because emphysema is manifested as low attenuation regions and intensity histograms represent different distributions for each type of emphysema. In our experiments, we evaluated several histogram lengths: $\{8, 16, 32\}$. However, the best results were achieved with 16-length histograms.

D. Feature ensemble

After computing the individual descriptors, a 38-length ensemble is built by concatenating the three different feature vectors one after another. This methodology is simple, yet effective and similar to [17] where the authors combined first and second order features using a fractal descriptor.

Theoretically, the more the features, the greater the ability to discriminate images. However, not all the features are important. Therefore, dimensionality reduction is performed using PCA. This reduction represents a normalization stage to prevent over-fitting. Here, we keep the first seven components that have the largest variance. This parameter was optimized based on the classification accuracy, namely, we tested and classified all the components. After the seventh component, the final classification rate declined around 5% and shows an oscillatory behavior. Hence, the reduced ensemble allows to characterize the emphysema information in a better way.

E. Classification

It is important that the method generalizes to unseen patients, thus, we applied leave-patient-out cross-validation and used random forest as a classifier.

Random forest classifier splits up the data in t trees. The idea is to grow a large number of trees, and at each node, get a different set of predictions and vote. We run the ensemble into the forest and obtained a prediction per tree. All those predictions are averaged together in order to get the predicted probabilities p of each class across every different tree. In general, the more trees the better the results. However, the classification rate decreases as the number of trees increases. According to [18], typical values of trees may vary from 16 to 128. We used $t = 32$, and we have found experimentally that increasing it further does not noticeably improve the accuracy.

IV. Experimental results

The dataset used here has been previously reported in [6] where the authors achieved an accuracy of 79.2% using LBPs, 61.3% with Gabor filters, and 95.2% with a combined model based on LBPs and intensity histograms. The methods were classified using k-NN. In [5], an average accuracy of 89.39% using LBPs, Gabor filters, and k-NN was reported. Azim et al. [9] used a kernel Fisher method and achieved an accuracy of 86.97%, whereas in [19], the authors shown an accuracy of 69.33%.

Our proposal achieved an accuracy of 91.07%. This result is shown in a confusion matrix in Fig. 4(a). We also included a classification using k-NN with $k = 1$, see Fig. 4(b).

It is worth saying that the reason that the NT patches were misclassified as PS is because most of the tissue in those NT ROIs belongs to the pleura. Since PS is localized around the pleura, the likelihood of being a diseased tissue is greater than being a healthy tissue.

Finally, we carried out a comparison between our proposal and all the single descriptors, the results are summarized in Table I.

V. Conclusions

We proposed a new approach for quantifying emphysema patterns based on an ensemble of features that allows to encode multi-scale textural characteristics and attenuation values. We also introduce the MDY descriptor that captures textural variations of emphysematous tissue. The classification results obtained as confusion matrices demonstrated that the feature ensemble can be used as a global descriptor. Based on the

Table I. COMPARISON AND CLASSIFICATION RESULTS OF EMPHYSEMATOUS TISSUE. SINCE THE STATISTICAL MEASURES ARE APPLICABLE TO A BINARY CLASSIFICATION, THEN WE COMPUTED ONE-VERSUS-ALL, AS IN [5]. ALL THE DATA ARE EXPRESSED IN (%). BOLD VALUES REPRESENT THE BEST RESULTS.

Method	Random Forest			*K*-NN		
	Precision	Sensitivity	Specificity	Precision	Sensitivity	Specificity
LGF	84.36	84.24	91.84	81.71	80.75	89.98
MDY	56.21	58.48	79.62	56.70	54.88	77.72
Histograms	66.65	66.89	83.74	65.77	65.20	82.73
Ensemble	**91.27**	**91.22**	**95.48**	80.51	80.64	90.12

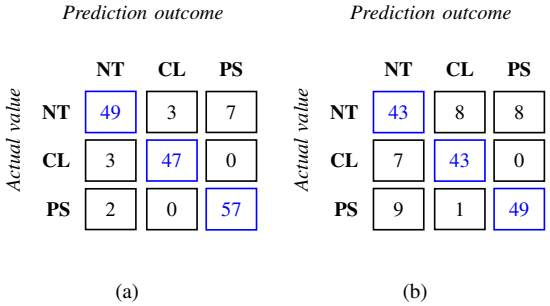

Figure 4. Confusion matrices of the proposed ensemble using **(a)** random forest and **(b)** k-NN classifiers. NT Normal tissue, CL Centrilobular emphysema, and PS Paraseptal emphysema.

results, it is clear that emphysema must be characterized by a combination of features because texture or intensity are not enough to describe the disease, (see Table I). Furthermore, the proposal has shown its ability to differentiate paraseptal from centrilobular emphysema regardless the classifier.

ACKNOWLEDGMENTS

The authors extend their gratitude to Prof. Dr. Marleen de Bruijne and Dr. Lauge Sørensen for providing the images. This publication was partially supported by the European social fund within the project CZ.1.07/2.3.00/30.0034, CTM-2014-51907, and UNAM PAPIIT grant IG100814. R. Nava and J. Olveres thank Consejo Nacional de Ciencia y Tecnología (CONACYT). J. Kybic was supported by the Czech Science Foundation project 14-21421S.

REFERENCES

[1] Global Initiative for Chronic Obstructive Lung Disease (GOLD). (2015) From the global strategy for the diagnosis, management and prevention of COPD. [Online]. Available: http://www.goldcopd.org/

[2] J. Al-Tubaikh, "Emphysema," in *Internal Medicine*, J. Al-Tubaikh, Ed. Springer Berlin Heidelberg, 2010, pp. 131–134.

[3] C. J. Galban, M. K. Han, J. L. Boes, K. A. Chughtai, C. R. Meyer, T. D. Johnson, S. Galban, A. Rehemtulla, E. A. Kazerooni, F. J. Martinez, and B. D. Ross, "Computed tomography-based biomarker provides unique signature for diagnosis of COPD phenotypes and disease progression," *Nat Med*, vol. 18, no. 11, pp. 1711–1715, 2012.

[4] N. Sverzellati, G. Randi, P. Spagnolo, A. Marchianò, M. Silva, J.-M. Kuhnigk, C. L. Vecchia, M. Zompatori, and U. Pastorino, "Increased mean lung density: another independent predictor of lung cancer?" *European Journal of Radiology*, vol. 82, no. 8, pp. 1325–1331, 2013.

[5] R. Nava, B. Escalante-Ramírez, G. Cristóbal, and R. S. J. Estépar, "Extended Gabor approach applied to classification of emphysematous patterns in computed tomography," *Medical & Biological Engineering & Computing*, vol. 52, no. 4, pp. 393–403, 2014.

[6] L. Sørensen, S. Shaker, and M. de Bruijne, "Quantitative analysis of pulmonary emphysema using local binary patterns," *IEEE Transactions on Medical Imaging*, vol. 29, no. 2, pp. 559–569, 2010.

[7] T. Ojala, M. Pietikäinen, and T. Maenpaa, "Multiresolution gray-scale and rotation invariant texture classification with local binary patterns," *IEEE Transactions on Pattern Analysis and Machine Intelligence*, vol. 24, no. 7, pp. 971–987, 2002.

[8] C. Dharmagunawardhana, S. Mahmoodi, M. Bennett, and M. Niranjan, "Quantitative analysis of pulmonary emphysema using isotropic Gaussian Markov random fields," in *Proceedings of the 9th International Conference on Computer Vision Theory and Applications, (VISAPP)*, 2014, pp. 44–53.

[9] T. Azim and M. Niranjan, "Texture classification with Fisher kernel extracted from the continuous models of RBM," in *Proceedings of the 9th International Conference on Computer Vision Theory and Applications, (VISAPP)*, 2014, pp. 684–690.

[10] F. Chabat, G.-Z. Yang, and D. M. Hansell, "Obstructive lung diseases: Texture classification for differentiation at CT," *Radiology*, vol. 228, no. 3, pp. 871–877, 2003.

[11] D. Hansell, A. Bankier, H. MacMahon, T. McLoud, N. Müller, and J. Remy, "Fleischner society: Glossary of terms for thoracic imaging," *Radiology*, vol. 3, no. 246, pp. 697–722, 2008.

[12] D. J. Field, "Relations between the statistics of natural images and the response properties of cortical cells," *J. Opt. Soc. Am. A*, vol. 4, no. 12, pp. 2379–2394, 1987.

[13] R. Andrle, "The angle measure technique: A new method for characterizing the complexity of geomorphic lines," *Mathematical Geology*, vol. 26, no. 1, pp. 83–97, 1994.

[14] R. Nava, B. Escalante-Ramírez, and G. Cristóbal, "A comparison study of Gabor and log-Gabor wavelets for texture segmentation," in *7th International Symposium on Image and Signal Processing and Analysis (ISPA)*, 2011, pp. 189–194.

[15] J. Huang and K. H. Esbensen, "Applications of angle measure technique (AMT) in image analysis: Part I. A new methodology for in situ powder characterization," *Chemometrics and Intelligent Laboratory Systems*, vol. 54, no. 1, pp. 1–19, 2000.

[16] P. Mendona, D. Padfield, J. Ross, J. Miller, S. Dutta, and S. Gautham, "Quantification of emphysema severity by histogram analysis of CT scans," in *Medical Image Computing and Computer-Assisted Intervention MICCAI 2005*, ser. Lecture Notes in Computer Science, J. Duncan and G. Gerig, Eds., 2005, vol. 3749, pp. 738–744.

[17] Y. Xu, M. Sonka, G. Mclennan, J. Guo, and E. Hoffman, "MDCT-based 3-D texture classification of emphysema and early smoking related lung pathologies," *IEEE Transactions on Medical Imaging*, vol. 25, no. 4, pp. 464–475, April 2006.

[18] T. M. Oshiro, P. S. Perez, and J. A. Baranauskas, "How many trees in a random forest?" in *Machine Learning and Data Mining in Pattern Recognition*, ser. Lecture Notes in Computer Science, P. Perner, Ed. Springer Berlin Heidelberg, 2012, vol. 7376, pp. 154–168.

[19] M. Ibrahim and R. Mukundan, "Multi-fractal techniques for emphysema classification in lung tissue images," in *3rd International Conference on Environment, Chemistry and Biology (ICECB)*, 2014, pp. 119–123.